Precise Measurement of the $e^+e^- \to \pi^+\pi^-(\gamma)$ Cross Section with the Initial State Radiation Method at *BABAR*

B. Aubert,[1] Y. Karyotakis,[1] J. P. Lees,[1] V. Poireau,[1] E. Prencipe,[1] X. Prudent,[1] V. Tisserand,[1] J. Garra Tico,[2] E. Grauges,[2] M. Martinelli,[3a,3b] A. Palano,[3a,3b] M. Pappagallo,[3a,3b] G. Eigen,[4] B. Stugu,[4] L. Sun,[4] M. Battaglia,[5] D. N. Brown,[5] B. Hooberman,[5] L. T. Kerth,[5] Yu. G. Kolomensky,[5] G. Lynch,[5] I. L. Osipenkov,[5] K. Tackmann,[5] T. Tanabe,[5] C. M. Hawkes,[6] N. Soni,[6] A. T. Watson,[6] H. Koch,[7] T. Schroeder,[7] D. J. Asgeirsson,[8] C. Hearty,[8] T. S. Mattison,[8] J. A. McKenna,[8] M. Barrett,[9] A. Khan,[9] A. Randle-Conde,[9] V. E. Blinov,[10] A. D. Bukin,[10,*] A. R. Buzykaev,[10] V. P. Druzhinin,[10] V. B. Golubev,[10] A. P. Onuchin,[10] S. I. Serednyakov,[10] Yu. I. Skovpen,[10] E. P. Solodov,[10] K. Yu. Todyshev,[10] M. Bondioli,[11] S. Curry,[11] I. Eschrich,[11] D. Kirkby,[11] A. J. Lankford,[11] P. Lund,[11] M. Mandelkern,[11] E. C. Martin,[11] D. P. Stoker,[11] H. Atmacan,[12] J. W. Gary,[12] F. Liu,[12] O. Long,[12] G. M. Vitug,[12] Z. Yasin,[12] V. Sharma,[13] C. Campagnari,[14] T. M. Hong,[14] D. Kovalskyi,[14] M. A. Mazur,[14] J. D. Richman,[14] T. W. Beck,[15] A. M. Eisner,[15] C. A. Heusch,[15] J. Kroseberg,[15] W. S. Lockman,[15] A. J. Martinez,[15] T. Schalk,[15] B. A. Schumm,[15] A. Seiden,[15] L. Wang,[15] L. O. Winstrom,[15] C. H. Cheng,[16] D. A. Doll,[16] B. Echenard,[16] F. Fang,[16] D. G. Hitlin,[16] I. Narsky,[16] P. Ongmongkolkul,[16] T. Piatenko,[16] F. C. Porter,[16] R. Andreassen,[17] G. Mancinelli,[17] B. T. Meadows,[17] K. Mishra,[17] M. D. Sokoloff,[17] P. C. Bloom,[18] W. T. Ford,[18] A. Gaz,[18] J. F. Hirschauer,[18] M. Nagel,[18] U. Nauenberg,[18] J. G. Smith,[18] S. R. Wagner,[18] R. Ayad,[19,†] W. H. Toki,[19] E. Feltresi,[20] A. Hauke,[20] H. Jasper,[20] T. M. Karbach,[20] J. Merkel,[20] A. Petzold,[20] B. Spaan,[20] K. Wacker,[20] M. J. Kobel,[21] R. Nogowski,[21] K. R. Schubert,[21] R. Schwierz,[21] D. Bernard,[22] E. Latour,[22] M. Verderi,[22] P. J. Clark,[23] S. Playfer,[23] J. E. Watson,[23] M. Andreotti,[24a,24b] D. Bettoni,[24a] C. Bozzi,[24a] R. Calabrese,[24a,24b] A. Cecchi,[24a,24b] G. Cibinetto,[24a,24b] E. Fioravanti,[24a,24b] P. Franchini,[24a,24b] E. Luppi,[24a,24b] M. Munerato,[24a,24b] M. Negrini,[24a,24b] A. Petrella,[24a,24b] L. Piemontese,[24a] V. Santoro,[24a,24b] R. Baldini-Ferroli,[25] A. Calcaterra,[25] R. de Sangro,[25] G. Finocchiaro,[25] S. Pacetti,[25] P. Patteri,[25] I. M. Peruzzi,[25,‡] M. Piccolo,[25] M. Rama,[25] A. Zallo,[25] R. Contri,[26a,26b] E. Guido,[26a,26b] M. Lo Vetere,[26a,26b] M. R. Monge,[26a,26b] S. Passaggio,[26a] C. Patrignani,[26a,26b] E. Robutti,[26a] S. Tosi,[26a,26b] M. Morii,[27] A. Adametz,[28] J. Marks,[28] S. Schenk,[28] U. Uwer,[28] F. U. Bernlochner,[29] H. M. Lacker,[29] T. Lueck,[29] A. Volk,[29] P. D. Dauncey,[30] M. Tibbetts,[30] P. K. Behera,[31] M. J. Charles,[31] U. Mallik,[31] J. Cochran,[32] H. B. Crawley,[32] L. Dong,[32] V. Eyges,[32] W. T. Meyer,[32] S. Prell,[32] E. I. Rosenberg,[32] A. E. Rubin,[32] Y. Y. Gao,[33] A. V. Gritsan,[33] Z. J. Guo,[33] N. Arnaud,[34] A. D'Orazio,[34] M. Davier,[34] D. Derkach,[34] J. Firmino da Costa,[34] G. Grosdidier,[34] F. Le Diberder,[34] V. Lepeltier,[34] A. M. Lutz,[34] B. Malaescu,[34] P. Roudeau,[34] M. H. Schune,[34] J. Serrano,[34] V. Sordini,[34,§] A. Stocchi,[34] L. L. Wang,[34,‖] G. Wormser,[34] D. J. Lange,[35] D. M. Wright,[35] I. Bingham,[36] J. P. Burke,[36] C. A. Chavez,[36] J. R. Fry,[36] E. Gabathuler,[36] R. Gamet,[36] D. E. Hutchcroft,[36] D. J. Payne,[36] C. Touramanis,[36] A. J. Bevan,[37] C. K. Clarke,[37] F. Di Lodovico,[37] R. Sacco,[37] M. Sigamani,[37] G. Cowan,[38] S. Paramesvaran,[38] A. C. Wren,[38] D. N. Brown,[39] C. L. Davis,[39] M. Fritsch,[40] W. Gradl,[40] A. Hafner,[40] K. E. Alwyn,[41] D. Bailey,[41] R. J. Barlow,[41] G. Jackson,[41] G. D. Lafferty,[41] T. J. West,[41] J. I. Yi,[41] J. Anderson,[42] C. Chen,[42] A. Jawahery,[42] D. A. Roberts,[42] G. Simi,[42] J. M. Tuggle,[42] C. Dallapiccola,[43] E. Salvati,[43] R. Cowan,[44] D. Dujmic,[44] P. H. Fisher,[44] S. W. Henderson,[44] G. Sciolla,[44] M. Spitznagel,[44] R. K. Yamamoto,[44] M. Zhao,[44] P. M. Patel,[45] S. H. Robertson,[45] M. Schram,[45] P. Biassoni,[46a,46b] A. Lazzaro,[46a,46b] V. Lombardo,[46a] F. Palombo,[46a,46b] S. Stracka,[46a,46b] L. Cremaldi,[47] R. Godang,[47,¶] R. Kroeger,[47] P. Sonnek,[47] D. J. Summers,[47] H. W. Zhao,[47] X. Nguyen,[48] M. Simard,[48] P. Taras,[48] H. Nicholson,[49] G. De Nardo,[50a,50b] L. Lista,[50a] D. Monorchio,[50a,50b] G. Onorato,[50a,50b] C. Sciacca,[50a,50b] G. Raven,[51] H. L. Snoek,[51] C. P. Jessop,[52] K. J. Knoepfel,[52] J. M. LoSecco,[52] W. F. Wang,[52] L. A. Corwin,[53] K. Honscheid,[53] H. Kagan,[53] R. Kass,[53] J. P. Morris,[53] A. M. Rahimi,[53] S. J. Sekula,[53] N. L. Blount,[54] J. Brau,[54] R. Frey,[54] O. Igonkina,[54] J. A. Kolb,[54] M. Lu,[54] R. Rahmat,[54] N. B. Sinev,[54] D. Strom,[54] J. Strube,[54] E. Torrence,[54] G. Castelli,[55a,55b] N. Gagliardi,[55a,55b] M. Margoni,[55a,55b] M. Morandin,[55a] M. Posocco,[55a] M. Rotondo,[55a] F. Simonetto,[55a,55b] R. Stroili,[55a,55b] C. Voci,[55a,55b] P. del Amo Sanchez,[56] E. Ben-Haim,[56] G. R. Bonneaud,[56] H. Briand,[56] J. Chauveau,[56] O. Hamon,[56] Ph. Leruste,[56] G. Marchiori,[56] J. Ocariz,[56] A. Perez,[56] J. Prendki,[56] S. Sitt,[56] L. Gladney,[57] M. Biasini,[58a,58b] E. Manoni,[58a,58b] C. Angelini,[59a,59b] G. Batignani,[59a,59b] S. Bettarini,[59a,59b] G. Calderini,[59a,59b,**] M. Carpinelli,[59a,59b,††] A. Cervelli,[59a,59b] F. Forti,[59a,59b] M. A. Giorgi,[59a,59b] A. Lusiani,[59a,59c] M. Morganti,[59a,59b] N. Neri,[59a,59b] E. Paoloni,[59a,59b] G. Rizzo,[59a,59b] J. J. Walsh,[59a] D. Lopes Pegna,[60] C. Lu,[60] J. Olsen,[60] A. J. S. Smith,[60] A. V. Telnov,[60] F. Anulli,[61a] E. Baracchini,[61a,61b] G. Cavoto,[61a] R. Faccini,[61a,61b] F. Ferrarotto,[61a] F. Ferroni,[61a,61b] M. Gaspero,[61a,61b] P. D. Jackson,[61a] L. Li Gioi,[61a] M. A. Mazzoni,[61a] S. Morganti,[61a] G. Piredda,[61a] F. Renga,[61a,61b] C. Voena,[61a] M. Ebert,[62] T. Hartmann,[62] H. Schröder,[62] R. Waldi,[62] T. Adye,[63] B. Franek,[63] E. O. Olaiya,[63] F. F. Wilson,[63] S. Emery,[64] L. Esteve,[64] G. Hamel de Monchenault,[64] W. Kozanecki,[64] G. Vasseur,[64]

Ch. Yèche,[64] M. Zito,[64] M. T. Allen,[65] D. Aston,[65] D. J. Bard,[65] R. Bartoldus,[65] J. F. Benitez,[65] R. Cenci,[65] J. P. Coleman,[65] M. R. Convery,[65] J. C. Dingfelder,[65] J. Dorfan,[65] G. P. Dubois-Felsmann,[65] W. Dunwoodie,[65] R. C. Field,[65] M. Franco Sevilla,[65] B. G. Fulsom,[65] A. M. Gabareen,[65] M. T. Graham,[65] P. Grenier,[65] C. Hast,[65] W. R. Innes,[65] J. Kaminski,[65] M. H. Kelsey,[65] H. Kim,[65] P. Kim,[65] M. L. Kocian,[65] D. W. G. S. Leith,[65] S. Li,[65] B. Lindquist,[65] S. Luitz,[65] V. Luth,[65] H. L. Lynch,[65] D. B. MacFarlane,[65] H. Marsiske,[65] R. Messner,[65,*] D. R. Muller,[65] H. Neal,[65] S. Nelson,[65] C. P. O'Grady,[65] I. Ofte,[65] M. Perl,[65] B. N. Ratcliff,[65] A. Roodman,[65] A. A. Salnikov,[65] R. H. Schindler,[65] J. Schwiening,[65] A. Snyder,[65] D. Su,[65] M. K. Sullivan,[65] K. Suzuki,[65] S. K. Swain,[65] J. M. Thompson,[65] J. Va'vra,[65] A. P. Wagner,[65] M. Weaver,[65] C. A. West,[65] W. J. Wisniewski,[65] M. Wittgen,[65] D. H. Wright,[65] H. W. Wulsin,[65] A. K. Yarritu,[65] C. C. Young,[65] V. Ziegler,[65] X. R. Chen,[66] H. Liu,[66] W. Park,[66] M. V. Purohit,[66] R. M. White,[66] J. R. Wilson,[66] M. Bellis,[67] P. R. Burchat,[67] A. J. Edwards,[67] T. S. Miyashita,[67] S. Ahmed,[68] M. S. Alam,[68] J. A. Ernst,[68] B. Pan,[68] M. A. Saeed,[68] S. B. Zain,[68] A. Soffer,[69] S. M. Spanier,[70] B. J. Wogsland,[70] R. Eckmann,[71] J. L. Ritchie,[71] A. M. Ruland,[71] C. J. Schilling,[71] R. F. Schwitters,[71] B. C. Wray,[71] B. W. Drummond,[72] J. M. Izen,[72] X. C. Lou,[72] F. Bianchi,[73a,73b] D. Gamba,[73a,73b] M. Pelliccioni,[73a,73b] M. Bomben,[74a,74b] L. Bosisio,[74a,74b] C. Cartaro,[74a,74b] G. Della Ricca,[74a,74b] L. Lanceri,[74a,74b] L. Vitale,[74a,74b] V. Azzolini,[75] N. Lopez-March,[75] F. Martinez-Vidal,[75] D. A. Milanes,[75] A. Oyanguren,[75] J. Albert,[76] Sw. Banerjee,[76] B. Bhuyan,[76] H. H. F. Choi,[76] K. Hamano,[76] G. J. King,[76] R. Kowalewski,[76] M. J. Lewczuk,[76] I. M. Nugent,[76] J. M. Roney,[76] R. J. Sobie,[76] T. J. Gershon,[77] P. F. Harrison,[77] J. Ilic,[77] T. E. Latham,[77] G. B. Mohanty,[77] E. M. T. Puccio,[77] H. R. Band,[78] X. Chen,[78] S. Dasu,[78] K. T. Flood,[78] Y. Pan,[78] R. Prepost,[78] C. O. Vuosalo,[78] and S. L. Wu[78]

(*BABAR* Collaboration)

[1]*Laboratoire d'Annecy-le-Vieux de Physique des Particules (LAPP), Université de Savoie, CNRS/IN2P3, F-74941 Annecy-Le-Vieux, France*
[2]*Universitat de Barcelona, Facultat de Fisica, Departament ECM, E-08028 Barcelona, Spain*
[3a]*INFN Sezione di Bari, Dipartimento di Fisica, I-70126 Bari, Italy*
[3b]*Università di Bari, I-70126 Bari, Italy*
[4]*University of Bergen, Institute of Physics, N-5007 Bergen, Norway*
[5]*Lawrence Berkeley National Laboratory and University of California, Berkeley, California 94720, USA*
[6]*University of Birmingham, Birmingham, B15 2TT, United Kingdom*
[7]*Ruhr Universität Bochum, Institut für Experimentalphysik 1, D-44780 Bochum, Germany*
[8]*University of British Columbia, Vancouver, British Columbia, Canada V6T 1Z1*
[9]*Brunel University, Uxbridge, Middlesex UB8 3PH, United Kingdom*
[10]*Budker Institute of Nuclear Physics, Novosibirsk 630090, Russia*
[11]*University of California at Irvine, Irvine, California 92697, USA*
[12]*University of California at Riverside, Riverside, California 92521, USA*
[13]*University of California at San Diego, La Jolla, California 92093, USA*
[14]*University of California at Santa Barbara, Santa Barbara, California 93106, USA*
[15]*University of California at Santa Cruz, Institute for Particle Physics, Santa Cruz, California 95064, USA*
[16]*California Institute of Technology, Pasadena, California 91125, USA*
[17]*University of Cincinnati, Cincinnati, Ohio 45221, USA*
[18]*University of Colorado, Boulder, Colorado 80309, USA*
[19]*Colorado State University, Fort Collins, Colorado 80523, USA*
[20]*Technische Universität Dortmund, Fakultät Physik, D-44221 Dortmund, Germany*
[21]*Technische Universität Dresden, Institut für Kern- und Teilchenphysik, D-01062 Dresden, Germany*
[22]*Laboratoire Leprince-Ringuet, CNRS/IN2P3, Ecole Polytechnique, F-91128 Palaiseau, France*
[23]*University of Edinburgh, Edinburgh EH9 3JZ, United Kingdom*
[24a]*INFN Sezione di Ferrara, Dipartimento di Fisica, I-44100 Ferrara, Italy*
[24b]*Università di Ferrara, I-44100 Ferrara, Italy*
[25]*INFN Laboratori Nazionali di Frascati, I-00044 Frascati, Italy*
[26a]*INFN Sezione di Genova, Dipartimento di Fisica, I-16146 Genova, Italy*
[26b]*Università di Genova, I-16146 Genova, Italy*
[27]*Harvard University, Cambridge, Massachusetts 02138, USA*
[28]*Universität Heidelberg, Physikalisches Institut, Philosophenweg 12, D-69120 Heidelberg, Germany*
[29]*Humboldt-Universität zu Berlin, Institut für Physik, Newtonstr. 15, D-12489 Berlin, Germany*
[30]*Imperial College London, London, SW7 2AZ, United Kingdom*
[31]*University of Iowa, Iowa City, Iowa 52242, USA*
[32]*Iowa State University, Ames, Iowa 50011-3160, USA*

[33]Johns Hopkins University, Baltimore, Maryland 21218, USA
[34]Laboratoire de l'Accélérateur Linéaire, IN2P3/CNRS et Université Paris-Sud 11, Centre Scientifique d'Orsay, B. P. 34, F-91898 Orsay Cedex, France
[35]Lawrence Livermore National Laboratory, Livermore, California 94550, USA
[36]University of Liverpool, Liverpool L69 7ZE, United Kingdom
[37]Queen Mary, University of London, London, E1 4NS, United Kingdom
[38]University of London, Royal Holloway and Bedford New College, Egham, Surrey TW20 0EX, United Kingdom
[39]University of Louisville, Louisville, Kentucky 40292, USA
[40]Johannes Gutenberg-Universität Mainz, Institut für Kernphysik, D-55099 Mainz, Germany
[41]University of Manchester, Manchester M13 9PL, United Kingdom
[42]University of Maryland, College Park, Maryland 20742, USA
[43]University of Massachusetts, Amherst, Massachusetts 01003, USA
[44]Massachusetts Institute of Technology, Laboratory for Nuclear Science, Cambridge, Massachusetts 02139, USA
[45]McGill University, Montréal, Québec, Canada H3A 2T8
[46a]INFN Sezione di Milano, Dipartimento di Fisica, I-20133 Milano, Italy
[46b]Università di Milano, I-20133 Milano, Italy
[47]University of Mississippi, University, Mississippi 38677, USA
[48]Université de Montréal, Physique des Particules, Montréal, Québec, Canada H3C 3J7
[49]Mount Holyoke College, South Hadley, Massachusetts 01075, USA
[50a]INFN Sezione di Napoli, Dipartimento di Scienze Fisiche, I-80126 Napoli, Italy
[50b]Università di Napoli Federico II, I-80126 Napoli, Italy
[51]NIKHEF, National Institute for Nuclear Physics and High Energy Physics, NL-1009 DB Amsterdam, The Netherlands
[52]University of Notre Dame, Notre Dame, Indiana 46556, USA
[53]Ohio State University, Columbus, Ohio 43210, USA
[54]University of Oregon, Eugene, Oregon 97403, USA
[55a]INFN Sezione di Padova, Dipartimento di Fisica, I-35131 Padova, Italy
[55b]Università di Padova, I-35131 Padova, Italy
[56]Laboratoire de Physique Nucléaire et de Hautes Energies, IN2P3/CNRS, Université Pierre et Marie Curie-Paris6, Université Denis Diderot-Paris7, F-75252 Paris, France
[57]University of Pennsylvania, Philadelphia, Pennsylvania 19104, USA
[58a]INFN Sezione di Perugia, Dipartimento di Fisica, I-06100 Perugia, Italy
[58b]Università di Perugia, I-06100 Perugia, Italy
[59a]INFN Sezione di Pisa, Dipartimento di Fisica, I-56127 Pisa, Italy
[59b]Università di Pisa, I-56127 Pisa, Italy
[59c]Scuola Normale Superiore di Pisa, I-56127 Pisa, Italy
[60]Princeton University, Princeton, New Jersey 08544, USA
[61a]INFN Sezione di Roma, Dipartimento di Fisica, I-00185 Roma, Italy
[61b]Università di Roma La Sapienza, I-00185 Roma, Italy
[62]Universität Rostock, D-18051 Rostock, Germany
[63]Rutherford Appleton Laboratory, Chilton, Didcot, Oxon, OX11 0QX, United Kingdom
[64]CEA, Irfu, SPP, Centre de Saclay, F-91191 Gif-sur-Yvette, France
[65]SLAC National Accelerator Laboratory, Stanford, California 94309 USA
[66]University of South Carolina, Columbia, South Carolina 29208, USA
[67]Stanford University, Stanford, California 94305-4060, USA
[68]State University of New York, Albany, New York 12222, USA
[69]Tel Aviv University, School of Physics and Astronomy, Tel Aviv, 69978, Israel
[70]University of Tennessee, Knoxville, Tennessee 37996, USA
[71]University of Texas at Austin, Austin, Texas 78712, USA
[72]University of Texas at Dallas, Richardson, Texas 75083, USA
[73a]INFN Sezione di Torino, Dipartimento di Fisica Sperimentale, I-10125 Torino, Italy
[73b]Università di Torino, I-10125 Torino, Italy
[74a]INFN Sezione di Trieste, Dipartimento di Fisica, I-34127 Trieste, Italy
[74b]Università di Trieste, I-34127 Trieste, Italy
[75]IFIC, Universitat de Valencia-CSIC, E-46071 Valencia, Spain
[76]University of Victoria, Victoria, British Columbia, Canada V8W 3P6
[77]Department of Physics, University of Warwick, Coventry CV4 7AL, United Kingdom
[78]University of Wisconsin, Madison, Wisconsin 53706, USA

(Received 27 August 2009; published 3 December 2009)

A precise measurement of the cross section of the process $e^+e^- \to \pi^+\pi^-(\gamma)$ from threshold to an energy of 3 GeV is obtained with the initial state radiation (ISR) method using 232 fb^{-1} of data collected

with the *BABAR* detector at e^+e^- center-of-mass energies near 10.6 GeV. The ISR luminosity is determined from a study of the leptonic process $e^+e^- \to \mu^+\mu^-\gamma(\gamma)$. The leading-order hadronic contribution to the muon magnetic anomaly calculated using the $\pi\pi$ cross section measured from threshold to 1.8 GeV is $(514.1 \pm 2.2(\text{stat}) \pm 3.1(\text{syst})) \times 10^{-10}$.

DOI: 10.1103/PhysRevLett.103.231801 PACS numbers: 13.66.Jn, 13.60.Hb, 13.66.Bc

Measurements of the $e^+e^- \to$ hadrons cross section are necessary to evaluate dispersion integrals for calculations of hadronic vacuum polarization (VP). Of particular interest is the contribution a_μ^{had} to the muon magnetic moment anomaly a_μ, which requires data in a region dominated by the process $e^+e^- \to \pi^+\pi^-(\gamma)$. Comparison of the theoretical and measured [1] values of a_μ shows a discrepancy of about 3σ when current e^+e^- data [2–4] are used, possibly hinting at new physics. An approach using τ decay data corrected for isospin breaking, leads to a smaller difference [5].

The results on $\pi\pi$ production reported in this Letter are obtained with the ISR method [6] using e^+e^- annihilation events collected at a center-of-mass (c.m.) energy $\sqrt{s}$ near 10.58 GeV. The cross section for $e^+e^- \to X$ at the reduced energy $\sqrt{s'} = m_X$, where X can be any final state, is deduced from a measurement of the radiative process $e^+e^- \to X\gamma$ where the photon is emitted by the e^+ or e^-; $s' = s(1 - 2E_\gamma^*/\sqrt{s})$, where E_γ^* is the c.m. energy of the ISR photon. In this analysis, $\sqrt{s'}$ ranges from threshold to 3 GeV. Two-body ISR processes with $X = \pi^+\pi^-(\gamma)$ and $X = \mu^+\mu^-(\gamma)$ are measured, where the ISR photon is detected at large angle and the charged-particle pair can be accompanied by a final state radiation (FSR) photon. Obtaining the $\pi\pi$ cross section from the ratio of pion to muon yield reduces significantly the systematic uncertainty. The measured muon cross section is compared to the QED prediction, and this cross check of the analysis is termed the QED test.

The $\sqrt{s'}$ spectrum of $e^+e^- \to X\gamma$ events is related to the cross section for the process $e^+e^- \to X$ through

$$\frac{dN_{X\gamma}}{d\sqrt{s'}} = \frac{dL_{\text{ISR}}^{\text{eff}}}{d\sqrt{s'}} \varepsilon_{X\gamma}(\sqrt{s'})\sigma_X^0(\sqrt{s'}), \quad (1)$$

where $\varepsilon_{X\gamma}$ is the detection efficiency (acceptance) determined by simulation with corrections obtained from data, and σ_X^0 is the bare cross section (excluding VP). The measurement of $\sigma^0_{\pi\pi(\gamma)}$ uses the effective ISR luminosity $dL_{\text{ISR}}^{\text{eff}}/d\sqrt{s'}$ provided by the measured mass spectrum of $\mu\mu\gamma(\gamma)$ events following Eq. (1) in which $\sigma_X^0(\sqrt{s'})$ is the $\mu\mu(\gamma)$ bare cross section computed with QED [7]. For the QED test, the measurement of $\sigma^0_{\mu\mu(\gamma)}$ uses the effective ISR luminosity definition as a product of the e^+e^- integrated luminosity (L_{ee}), the radiator function [6], the ratio of detection efficiencies for the ISR photon in data and simulation (not included in $\varepsilon_{X\gamma}$), and the VP correction $(\alpha(s')/\alpha(0))^2$. The radiator function, determined by the simulation, is the probability to radiate one or several ISR photons so that the produced final state X (excluding ISR photons) has mass $\sqrt{s'}$.

This analysis is based on 232 fb^{-1} of data recorded with the *BABAR* detector [8] at the PEP-II asymmetric-energy e^+e^- storage rings. Charged-particle tracks are measured with a five-layer double-sided silicon vertex tracker (SVT) together with a 40-layer drift chamber (DCH) inside a 1.5 T superconducting solenoid magnet. The energy and direction of photons are measured in the CsI(Tl) electromagnetic calorimeter (EMC). Charged-particle identification (PID) uses ionization loss dE/dx in the SVT and DCH, the Cherenkov radiation detected in a ring-imaging device (DIRC), and the shower deposit in the EMC (E_{cal}) and in the instrumented flux return (IFR) of the magnet.

Signal and background ISR processes are simulated with Monte Carlo (MC) event generators based on Ref. [9]. Additional ISR photons are generated with the structure function method [10], and additional FSR photons with PHOTOS [11]. Background events from $e^+e^- \to q\bar{q}$ ($q = u, d, s, c$) are generated with JETSET [12]. The response of the *BABAR* detector is simulated with GEANT4 [13].

Two-body ISR events are selected by requiring a photon with $E_\gamma^* > 3$ GeV and laboratory polar angle in the range 0.35–2.4 rad, and exactly two tracks of opposite charge, each with momentum $p > 1$ GeV/c and within the angular range 0.40–2.45 rad. If several photons are detected, the ISR photon is chosen to be that with the highest E_γ^*. The charged-particle tracks, required to have at least 15 hits in the DCH, must originate within 5 mm of the collision axis and extrapolate to DIRC and IFR active areas which exclude low-efficiency regions. An additional criterion based on a combination of E_{cal} and dE/dx reduces electron contamination.

Acceptance and mass-dependent efficiencies for trigger, reconstruction, PID, and event selection are computed using the simulation. The ratios of data and MC efficiencies have been determined from specific studies, as described below, and are applied as mass-dependent corrections to the MC efficiency. They amount to at most a few percent and are known to a few permil level or better.

Tracking and PID efficiencies are determined taking advantage of pair production. For tracking studies, two-prong ISR candidates are selected on the basis of the ISR photon and one track. A kinematic fit yields the expected parameters of the second track. The unbiased sample of candidate second tracks is used to measure track reconstruction efficiency. The maximum correlated two-track loss induced by track overlap in the DCH is 0.6% for pions and 0.3% for muons.

Tracks are assigned uniquely to a complete set of PID classes using a combination of cut-based and likelihood selectors. The 'μ' class is addressed first by making use of track IFR penetration and hit spread distribution, and of the $E_{\rm cal}$ value. Tracks failing the 'μ' identification are labeled as 'e' if they satisfy $E_{\rm cal}/p > 0.8$. The 'K' class is determined using DIRC information and dE/dx. Remaining tracks are labeled as 'π.' A tighter selection called 'π_h' is applied in mass regions where background dominates or to create a pure pion test sample.

Efficiencies for PID are measured from pure samples of muon, pion, and kaon pairs obtained from $x\bar{x}\gamma$ events where one track is selected as 'μ', 'π_h', or 'K', and the other is used to probe the PID algorithm. The efficiencies are stored according to momentum and position in the IFR or the DIRC. The typical efficiency for 'μ' is 90%, with 10% mis-ID as 'π.' The 'π' efficiency is strongly momentum dependent because of mis-ID as 'K' (1% at 1 GeV/c, reaching 20% at 6 GeV/c), as 'μ' (5%–6%), or as 'e' (2%).

To obtain the spectra N_{jj} of produced particle pairs of true type j, a set of three linear relations must be solved. They involve the N_{jj}, the measured mass distributions for each 'ii'-identified final state, and the probabilities $\varepsilon^{jj}_{ii'}$ (i, $j = \mu$, π or K) which represent the product of the measured efficiencies for each track of true type j to be identified as 'i'. Correlations between the PID efficiencies of the two tracks, due their overlap, have been observed and parametrized. They are largest for muons where the correlated PID loss reaches 1.3% of the events below 1 GeV/c^2. It is important to control this effect, since it affects the $\pi\pi$ and $\mu\mu$ samples in an anticorrelated way.

A contribution ($< 10^{-3}$) to $N_{\pi\pi}$ from $p\bar{p}\gamma$ is estimated from MC simulations and subtracted after reweighting the rate to agree with the *BABAR* measurement [14]. Multihadronic background from $e^+e^- \to q\bar{q}$ comes from low-multiplicity events in which an energetic γ originating from a π^0 is mistaken as the ISR photon candidate. To normalize this rate from JETSET, the π^0 yield obtained by pairing the ISR photon with other photons in the event is compared in data and MC simulations; JETSET overestimates this background by a factor 1.3. Multihadronic ISR backgrounds are dominated by $e^+e^- \to \pi^+\pi^-\pi^0\gamma$ and $e^+e^- \to \pi^+\pi^- 2\pi^0\gamma$ contributions which are estimated using resonance-based MC generators. An approach similar to that for $q\bar{q}$ is followed to calibrate the background level from the 3π ISR process, using ω and ϕ signals. The ratio of data to MC yield is found to be 0.99 ± 0.04. The MC estimate for the $2\pi 2\pi^0\gamma$ process is used and assigned a 10% systematic uncertainty. A residual radiative Bhabha background is identifiable only near threshold and at large mass, where the pion signal vanishes. Its magnitude is estimated from the distribution of the angle between the π^+ and the ISR photon in the $\pi\pi$ c.m. frame at low energy and its energy dependence obtained from a control sample of radiative Bhabha events. It is assigned a 100% systematic uncertainty. To suppress the contribution from the $e^+e^- \to \gamma\gamma$ process with a photon conversion, which affects the spectrum at threshold, the vertex of the two tracks is required to be closer than 5 mm to the collision axis in the transverse plane. This criterion is applied only to events in the ρ tails, defined to lie outside the central region $0.5 < m_{\pi\pi} < 1.0$ GeV/c^2. Background contributions to the $N_{\mu\mu}$ spectrum are negligible.

Each event is subjected to two kinematic fits to the $e^+e^- \to X\gamma$ hypothesis, where X includes one additional photon, detected or not. Both fits use the ISR photon direction and the parameters and covariance matrix of each charged-particle track. The energy of the ISR photon is not used, as it has little impact for the relatively low c.m. energies involved. The two-constraint (2C) "ISR" fit allows an undetected photon collinear with the collision axis, while the 3C "FSR" fit uses any photon with $E_\gamma > 25$ MeV. When more than one such photon is present, the best FSR fit is retained. An event with no extra photon is characterized only by its $\chi^2_{\rm ISR}$ value. Most events have small χ^2 values for both fits; an event with only a small $\chi^2_{\rm ISR}$ ($\chi^2_{\rm FSR}$) indicates the presence of additional ISR (FSR) radiation. Events where both fits have large χ^2 values result from track or ISR photon resolution effects, the presence of additional radiated photons, or multihadronic background. To accommodate the expected background levels, different criteria in the ($\chi^2_{\rm ISR}$, $\chi^2_{\rm FSR}$) plane are applied depending on the $m_{\pi\pi}$ mass regions. For the central ρ region, a loose 2D contour has been optimized to remove the main background area while maintaining control of the associated systematic uncertainties. The same procedure is used in the $\mu\mu\gamma$ analysis in spite of the very small background. In the ρ tails, a tighter χ^2 selection is imposed to reduce the larger background. Samples of 529320 pion and 445631 muon events are selected in the mass range below 3 GeV/c^2, where the $m_{\pi\pi}$ ($m_{\mu\mu}$) mass is calculated from the best ISR or FSR fit.

The computed acceptance and the χ^2 selection efficiency depend on the description of radiative effects in the generator. The FSR rate is measured from events that satisfy the FSR fit, with an additional photon ($E_\gamma > 0.2$ GeV) within 20° of either track. The excess in data relative to the generator prediction using PHOTOS [11] is $(-4 \pm 6)\%$ of total FSR for muons, and $(21 \pm 5)\%$ for pions. This difference results in a $(6 \pm 2) \times 10^{-4}$ correction. More significant differences are found between data and the generator for additional ISR photons, since the latter uses a collinear approximation and an energy cutoff for very hard photons. Induced kinematical effects have been studied using the next-to-leading-order (NLO) PHOKHARA generator [15] at the four-vector level with fast simulation. Differences in acceptance occur at the few percent level, and these yield corrections to the QED test. In contrast, since radiation from the initial state is

common to the pion and muon channels, the $\pi\pi(\gamma)$ cross section, obtained from the $\pi\pi/\mu\mu$ ratio, is affected and corrected only at a few permil level. Additional ISR effects on the χ^2 selection efficiencies factorize in both processes and cancel in the ratio. The χ^2 selection efficiency determined from muon data applies to pions, after correction for the effect of secondary interactions and the π/μ difference for additional FSR. Therefore, the measurement of the pion cross section is to a large extent insensitive to the description of NLO effects in the generator.

The QED test involves two additional factors, both of which cancel in the $\pi\pi/\mu\mu$ ratio: L_{ee} and the ISR photon efficiency, which is measured using a $\mu\mu\gamma$ sample selected only on the basis of the two muon tracks. The QED test is expressed as the ratio of data to the simulated spectrum, after the latter is corrected using data for all known detector and reconstruction differences. The generator is also corrected for its known NLO deficiencies using the comparison to PHOKHARA. The ratio is consistent with unity from threshold to 3 GeV/c^2, [Fig. 1(a)]. A fit to a constant value yields ($\chi^2/n_{\rm df} = 55.4/54$; $n_{\rm df}$ = number of degrees of freedom)

$$\frac{\sigma^{\rm data}_{\mu\mu\gamma(\gamma)}}{\sigma^{\rm NLO\ QED}_{\mu\mu\gamma(\gamma)}} - 1 = (40 \pm 20 \pm 55 \pm 94) \times 10^{-4}, \qquad (2)$$

where the errors are statistical, systematic from this analysis, and systematic from L_{ee} (measured using Bhabha scattering events), respectively. The QED test is thus satisfied within an overall accuracy of 1.1%.

To correct for resolution and FSR effects, an unfolding of the background-subtracted and efficiency-corrected $m_{\pi\pi}$ distribution is performed. A separate mass-transfer matrix is created using simulation for the ρ central and tail regions; this provides the probability that an event generated in a $\sqrt{s'}$ interval i is reconstructed in a $m_{\pi\pi}$ interval j. The matrix is corrected to account for the larger fraction of events with bad χ^2 values (and consequently poorer mass resolution) in data compared to the MC simulation because of the approximate simulation of additional ISR. The performance and robustness of the unfolding method [16] have been assessed using test models. For the 2-MeV intervals, the significant elements of the resulting covariance matrix lie near the diagonal over a typical range of 6–8 MeV, which corresponds to the energy resolution.

The results for the $e^+e^- \to \pi^+\pi^-(\gamma)$ bare cross section [17] including FSR, $\sigma^0_{\pi\pi(\gamma)}(\sqrt{s'})$, are given in Fig. 1(b). Prominent features are the dominant ρ resonance, the abrupt drop at 0.78 GeV due to $\rho - \omega$ interference, a clear dip at 1.6 GeV resulting from higher ρ state interference, and some additional structure near 2.2 GeV. Systematic uncertainties are estimated from the precision of the data-MC comparisons and from the measurement procedures used for the various efficiencies. They are reported in Table I for $0.3 < \sqrt{s'} < 1.2$ GeV. Although larger outside this range, the systematic uncertainties do not exceed statistical errors over the full spectrum for the chosen energy intervals.

The lowest-order contribution of the $\pi\pi(\gamma)$ intermediate state to the muon magnetic anomaly is given by

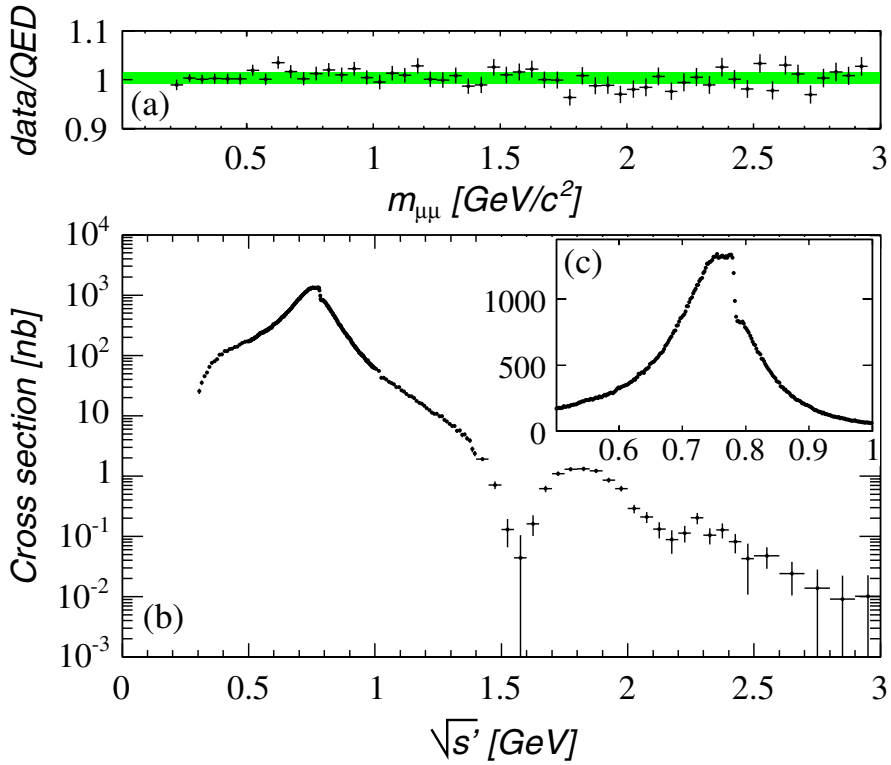

FIG. 1 (color online). (a) The ratio of the measured cross section for $e^+e^- \to \mu^+\mu^-\gamma(\gamma)$ to the NLO QED prediction. The band represents Eq. (2). (b) The measured cross section for $e^+e^- \to \pi^+\pi^-(\gamma)$ from 0.3 to 3 GeV. (c) Enlarged view of the ρ region in energy intervals of 2 MeV. The plotted errors are from the sum of the diagonal elements of the statistical and systematic covariance matrices.

TABLE I. Relative systematic uncertainties (in 10^{-3}) on the $e^+e^- \to \pi^+\pi^-(\gamma)$ cross section by $\sqrt{s'}$ intervals (in GeV) up to 1.2 GeV. The statistical part of the efficiency uncertainties is included in the total statistical uncertainty in each interval.

Source of uncertainty	$\sqrt{s'}$ (GeV) 0.3–0.4	0.4–0.5	0.5–0.6	0.6–0.9	0.9–1.2
Trigger/filter	5.3	2.7	1.9	1.0	0.5
Tracking	3.8	2.1	2.1	1.1	1.7
π-ID	10.1	2.5	6.2	2.4	4.2
Background	3.5	4.3	5.2	1.0	3.0
Acceptance	1.6	1.6	1.0	1.0	1.6
Kinematic fit (χ^2)	0.9	0.9	0.3	0.3	0.9
Correlated $\mu\mu$ ID loss	3.0	2.0	3.0	1.3	2.0
$\pi\pi/\mu\mu$ noncancel.	2.7	1.4	1.6	1.1	1.3
Unfolding	1.0	2.7	2.7	1.0	1.3
ISR luminosity ($\mu\mu$)	3.4	3.4	3.4	3.4	3.4
Total uncertainty	13.8	8.1	10.2	5.0	6.5

$$a_\mu^{\pi\pi(\gamma),\mathrm{LO}} = \frac{1}{4\pi^3}\int_{4m_\pi^2}^{\infty} ds' K(s')\sigma^0_{\pi\pi(\gamma)}(s'), \qquad (3)$$

where $K(s')$ is a known kernel [18]. The integration uses the measured cross section and the errors are computed using the full statistical and systematic covariance matrices. The systematic uncertainties for each source are taken to be fully correlated over all mass regions. The integrated result from threshold to 1.8 GeV is

$$a_\mu^{\pi\pi(\gamma),\mathrm{LO}} = (514.1 \pm 2.2 \pm 3.1) \times 10^{-10}, \qquad (4)$$

where the errors are statistical and systematic. This value is larger than that from a combination of previous e^+e^- data [5] (503.5 ± 3.5), but is in good agreement with the updated value from τ decay [5] (515.2 ± 3.4).

In summary, the cross section for the process $e^+e^- \to \pi^+\pi^-(\gamma)$ has been measured in the energy range from 0.3 to 3 GeV, using the ISR method. The result for the $\pi\pi$ hadronic contribution to a_μ has a precision comparable to that of the combined value from existing e^+e^- experiments. However, the *BABAR* central value is larger, which reduces the deviation of the direct a_μ measurement from the standard model prediction.

We are grateful for the excellent luminosity and machine conditions provided by our PEP-II colleagues, and for the substantial dedicated effort from the computing organizations that support *BABAR*. The collaborating institutions wish to thank SLAC for its support and kind hospitality. This work is supported by DOE and NSF (USA), NSERC (Canada), CEA and CNRS-IN2P3 (France), BMBF and DFG (Germany), INFN (Italy), FOM (The Netherlands), NFR (Norway), MES (Russia), MEC (Spain), and STFC (United Kingdom). Individuals have received support from the Marie Curie EIF (European Union) and the A. P. Sloan Foundation.

*Deceased.
†Present address: Temple University, Philadelphia, PA 19122, USA.
‡Also with Università di Perugia, Dipartimento di Fisica, Perugia, Italy.
§Also with Università di Roma La Sapienza, I-00185 Roma, Italy.
‖Also with Institute of High Energy Physics, Academy of Sciences, Beijing, China.
¶Now at University of South Alabama, Mobile, AL 36688, USA.
**Also with Laboratoire de Physique Nucléaire et de Hautes Energies, IN2P3/CNRS, Université Pierre et Marie Curie-Paris6, Université Denis Diderot-Paris7, F-75252 Paris, France.
††Also with Università di Sassari, Sassari, Italy.

[1] G. W. Bennett *et al.*, Phys. Rev. D **73**, 072003 (2006).
[2] V. M. Aulchenko *et al.*, JETP Lett. **82**, 743 (2005); JETP Lett. **84**, 413 (2006); R. R. Akhmetshin *et al.*, Phys. Lett. B **648**, 28 (2007).
[3] M. N. Achasov *et al.*, JETP **103**, 380 (2006).
[4] F. Ambrosino *et al.*, Phys. Lett. B **670**, 285 (2009).
[5] M. Davier *et al.*, arXiv:0906.5443 [Eur. Phys. J. (to be published)].
[6] A. B. Arbuzov *et al.*, J. High Energy Phys. 12 (1998) 009; S. Binner, J. H. Kühn, and K. Melnikov, Phys. Lett. B **459**, 279 (1999).
[7] Correction for the effect of lowest-order FSR is applied.
[8] B. Aubert *et al.*, Nucl. Instrum. Methods Phys. Res., Sect. A **479**, 1 (2002).
[9] H. Czyż and J. H. Kühn, Eur. Phys. J. C **18**, 497 (2001).
[10] M. Caffo, H. Czyż, and E. Remiddi, Nuovo Cimento A **110**, 515 (1997).
[11] E. Barberio, B. van Eijk, and Z. Was, Comput. Phys. Commun. **66**, 115 (1991).
[12] T. Sjöstrand, Comput. Phys. Commun. **82**, 74 (1994).
[13] S. Agostinelli *et al.*, Nucl. Instrum. Methods Phys. Res., Sect. A **506**, 250 (2003).
[14] B. Aubert *et al.*, Phys. Rev. D **73**, 012005 (2006).
[15] H. Czyż *et al.*, Eur. Phys. J. C **35**, 527 (2004); Eur. Phys. J. C **39**, 411 (2005).
[16] B. Malaescu, arXiv:0907.3791 [Nucl. Instrum. Methods (to be published)].
[17] See EPAPS Document No. E-PRLTAO-103-045950 for a file containing the cross section data, the full table of systematic errors and the statistical covariance matrix. For more information on EPAPS, see http://www.aip.org/pubservs/epaps.html.
[18] S. J. Brodsky and E. de Rafael, Phys. Rev. **168**, 1620 (1968).